NASA/TM-20250006527

Assessment of Thermoplastic Composite Joining by Resistance, Induction, and Ultrasonic Welding

Sandi G. Miller and Joseph J. Pinakidis
Glenn Research Center, Cleveland, Ohio

Paula J. Heimann
Universities Space Research Association, Cleveland, Ohio

Andrew C. Bergan, Patrick H. Johnston, Frank Leone, and Ji Su
Langley Research Center, Hampton, Virginia

Kenneth N. Segal
Intuitive Machines, Inc., Houston, Texas

William Mulhearn
Goddard Space Flight Center, Greenbelt, Maryland

John Chiu
Actalent, Hanover, Maryland

Waruna Seneviratne, Mark Walthers, and Upul Palliyaguru
National Institute of Aviation Research, Wichita, Kansas

Samuel Slater and Mark Wadsworth
Spirit Aerosystems, Wichita, Kansas

John Hertel, Chris Skocik, and Jim Stratton
Agile Ultrasonics, Columbus, Ohio

July 2025

NASA STI Program Report Series

Since its founding, NASA has been dedicated to the advancement of aeronautics and space science. The NASA scientific and technical information (STI) program plays a key part in helping NASA maintain this important role.

The NASA STI program operates under the auspices of the Agency Chief Information Officer. It collects, organizes, provides for archiving, and disseminates NASA's STI. The NASA STI program provides access to the NTRS Registered and its public interface, the NASA Technical Reports Server, thus providing one of the largest collections of aeronautical and space science STI in the world. Results are published in both non-NASA channels and by NASA in the NASA STI Report Series, which includes the following report types:

- TECHNICAL PUBLICATION.
  Reports of completed research or a major significant phase of research that present the results of NASA programs and include extensive data or theoretical analysis. Includes compilations of significant scientific and technical data and information deemed to be of continuing reference value. NASA counterpart of peer-reviewed formal professional papers but has less stringent limitations on manuscript length and extent of graphic presentations.

- TECHNICAL MEMORANDUM.
  Scientific and technical findings that are preliminary or of specialized interest, e.g., quick release reports, working papers, and bibliographies that contain minimal annotation. Does not contain extensive analysis.

- CONTRACTOR REPORT.
  Scientific and technical findings by NASA-sponsored contractors and grantees.

- CONFERENCE PUBLICATION.
  Collected papers from scientific and technical conferences, symposia, seminars, or other meetings sponsored or cosponsored by NASA.

- SPECIAL PUBLICATION.
  Scientific, technical, or historical information from NASA programs, projects, and missions, often concerned with subjects having substantial public interest.

- TECHNICAL TRANSLATION.
  English-language translations of foreign scientific and technical material pertinent to NASA's mission.

Specialized services also include organizing and publishing research results, distributing specialized research announcements and feeds, providing information desk and personal search support, and enabling data exchange services.

For more information about the NASA STI program, see the following:

- Access the NASA STI program home page at http://www.sti.nasa.gov

NASA/TM-20250006527

Assessment of Thermoplastic Composite Joining by Resistance, Induction, and Ultrasonic Welding

Sandi G. Miller and Joseph J. Pinakidis
Glenn Research Center, Cleveland, Ohio

Paula J. Heimann
Universities Space Research Association, Cleveland, Ohio

Andrew C. Bergan, Patrick H. Johnston, Frank Leone, and Ji Su
Langley Research Center, Hampton, Virginia

Kenneth N. Segal
Intuitive Machines, Inc., Houston, Texas

William Mulhearn
Goddard Space Flight Center, Greenbelt, Maryland

John Chiu
Actalent, Hanover, Maryland

Waruna Seneviratne, Mark Walthers, and Upul Palliyaguru
National Institute of Aviation Research, Wichita, Kansas

Samuel Slater and Mark Wadsworth
Spirit Aerosystems, Wichita, Kansas

John Hertel, Chris Skocik, and Jim Stratton
Agile Ultrasonics, Columbus, Ohio

National Aeronautics and
Space Administration

Glenn Research Center
Cleveland, Ohio 44135

July 2025

Level of Review: This material has been technically reviewed by technical management.

This report is available in electronic form at https://www.sti.nasa.gov/ and https://ntrs.nasa.gov/

NASA STI Program/Mail Stop 050
NASA Langley Research Center
Hampton, VA 23681-2199

Assessment of Thermoplastic Composite Joining by Resistance, Induction, and Ultrasonic Welding

Sandi G. Miller and Joseph J. Pinakidis
National Aeronautics and Space Administration
Glenn Research Center
Cleveland, Ohio 44135

Paula J. Heimann
Universities Space Research Association
Cleveland, Ohio 44135

Andrew C. Bergan, Patrick H. Johnston, Frank Leone, and Ji Su
National Aeronautics and Space Administration
Langley Research Center
Hampton, Virginia 23681–2199

Kenneth N. Segal
Intuitive Machines, Inc.
Houston, Texas 77059

William Mulhearn
National Aeronautics and Space Administration
Goddard Space Flight Center
Greenbelt, Maryland 20771

John Chiu
Actalent
Hanover, Maryland 21076

Waruna Seneviratne, Mark Walthers, and Upul Palliyaguru
National Institute of Aviation Research
Wichita, Kansas 67260

Samuel Slater and Mark Wadsworth
Spirit Aerosystems
Wichita, Kansas 67260

John Hertel, Chris Skocik, and Jim Stratton
Agile Ultrasonics
Columbus, Ohio 43212

Abstract

The NASA Game Changing Development (GCD) program, Thermoplastic Development for Exploration Applications (TDEA) project was initiated to advance NASA's capabilities to manufacture, model, and design with thermoplastic composites in support of future exploration missions. Recognizing that joints are a challenge area in many NASA applications using thermoset matrix composites, the project worked to develop structurally efficient joints for large scale thermoplastic composite space structures.

Thermoplastic composites are well suited for manufacturing large, lightweight aerospace structures through fusion bonding processes. Fusion bonding, or welding, refers to heating a thermoplastic joint at the bondline, providing time and pressure as required for polymer chain reptation across the weld interface, and cooling under pressure to solidify the joint. Several methods for welding thermoplastic composites are available however the three often used in aerospace include resistance, induction, and ultrasonic welding. The goal of this work is to evaluate the requirements, benefits, and constraints of these three welding methods to join four candidate thermoplastic composite material systems. Lap shear coupons were welded by each method on a per coupon basis. The weld area was limited to the 2.54 by 2.54 cm coupon overlap region to provide an assessment of the reproducibility of each weld process and the influence of edge effects. The outcome of this work includes the apparent lap shear strength of each material and weld method, an assessment of the reproducibility of lap shear strength produced by each method, material effects, and examination of edge effects through non-destructive evaluation.

Introduction

Application of thermoplastic composites for space structures has been considered since at least 1978 with a Boeing report comparing the structural properties, manufacturability, and repairability of thermoplastic composites with epoxy-based composites (Ref. 1). In the 1980s Boeing also evaluated thermoplastic matrix composites with pitch-based carbon fiber for use in satellites, where stiffness and coefficient of thermal expansion (CTE) requirements are critical (Ref. 2). In 1990, Oak Ridge National Lab released a paper which compared graphite/polyether ether ketone (PEEK) and graphite/epoxy with respect to material properties relevant to space applications. These included water absorption, out-gassing, space-environment effects, dimensional stability, and joining alternatives. In all cases the thermoplastic outperformed epoxy (Ref. 3).

More recently, the European Space Agency (ESA) has evaluated materials, manufacturing, and joining methods for space structures including thermoplastic composite propellant tanks and launch vehicles (Refs. 4 to 6). ESA has evaluated thermoplastic composites to manufacture an integrally-stiffened curved panel which was based on the design of the 2/3 interstage of the Ariane 4 space launcher (Ref. 7). The German Aerospace Center is currently developing a carbon fiber/PEEK primary structure for a sounding rocket (Ref. 4). The 2015 NASA-JPL Soil Moisture Active/Passive (SMAP) satellite utilized an aramid fiber and polyetherimide (PEI) matrix structure for the deployable AstroMesh Lite reflector (Ref. 8) and NASA has evaluated in-space manufacturing of thermoplastic structures through a 3D printing process with both continuous and chopped (Refs. 9 and 10).

While thermoplastic composite materials have been evaluated for and flown on space structures, less emphasis has been placed on joining either conventional structural applications that would be terrestrially assembled and launched into space, or novel structural applications designed for in-space assembly through joining processes. Several joining techniques have been developed to bond thermoplastic composites (primarily for aeronautical applications, e.g., (Refs. 11 and 12) with the heat source being the primary differentiator. In general, welding, or fusion bonding refers to a joining process where two contacting thermoplastic parts are fused together by heating the polymer at the interface to a molten state, intermolecular diffusion and reptation across the bond interface, and then solidification on cooling. When full entanglement and ideal uniform recrystallization occurs (for semi-crystalline polymers), the joint is indistinguishable from the parent material (Ref. 13). In this paper, the term welding will be used to describe thermoplastic joining through a fusion bonding process.

Resistance welding (RW), induction welding (IW), and ultrasonic welding (UW) are three common welding methods with distinct benefits and limitations in practice. The selection of which joining process to use is dependent the materials, component complexity, and design constraints of the bonded structure. This study assessed RW, IW, and UW to select a process most applicable to welding a repeating truss structure where the influence of edge effects would be significant. The characteristics, advantages, and challenges of each method are summarized in Table I.

TABLE I.—CHARACTERISTICS OF COMMON WELDING PROCESSES FOR THERMOPLASTIC COMPOSITES

	Welding method		
	Resistance	Induction	Ultrasonic
Heat Source	Joule heating from resistive element positioned at the bondline.	Induction induces eddy currents in carbon fiber adherends or conductive susceptor which absorbs electromagnetic energy and in turn produces Joule heating.	Bulk and interface friction from ultrasonic vibration.
Material Forms/ Limitations	Resistive element remains within part acting as stress riser within bond line. In addition, CTE mismatch of the additional material poses a challenge for space applications. Requires tooling and heat management systems for uniform pressure and temperature control across the full bond line. Current leakage increases power requirement and can lead to heating outside the bondline.	Best suited for cross-ply or braids which do not require an insert at the interface). Otherwise, additional material may be required at the interface leading to concerns similar to resistance welding. Requires tooling and heat management systems for uniform pressure and temperature control across the full bond line. Welding near trimmed edges requires additional provisions to mitigate excessive current generation.	Energy director is often required which is typically the resin material itself molded to include rough features such as a pyramid or mesh. There has been work to evaluate the weld without an energy director. Cooling rate can be very high making it difficult to achieve high degree of crystallinity. Distortional defects can occur, especially near substrate edges. Boundary conditions are important to isolate the vibrational energy.
Advantages	Rapid heating of bond interface only, as opposed to heating from the joint surface.	Noncontact heating. Well suited for long continuous welds. Can weld with no additional material at weld interface. Potentially allows for geometrically complex welds.	Spot welding, current development into continuous 'scan' welds reported in the literature and welding without an energy director.
Current Applications and Active Development	Has been established as the method used for joining ribs to the skin of the Airbus A340 and A380 wing leading edges. Continuous welding developed as part of the Multi-Functional Fuselage Demonstrator (MFFD).	GKN Fokker Aerostructures and Gulfstream used induction welding technology for assembly of the empennage control surfaces in the G650 business jet aircraft.	The method has been demonstrated by Lockheed-Georgia to weld together thermoplastic/graphite tape material for the C-130 Hercules aircraft. CleanSky program- continuous ultrasonic welding for attachment of stringers to the fuselage skin- demonstrator vehicle.

Similar reports are available that compare welding processes for thermoplastic composites (Refs. 14 to 22). Villegas et al. details process variables such as weld time and required power and energy for carbon fiber/PPS composites welded by induction, resistance, and ultrasonic welding (Ref. 23). Ageorges and Ye provide an overview of fusion bonding which summarizes the benefits and limitations of these three welding processes with respect to reproducibility, flexibility, and large-scale joining among other metrics (Ref. 24). More recently, Korycki et al. presents a comparative analysis of ultrasonic, induction, and through transmission laser welding methods to join CF/PEEK. The advantages and drawbacks of each process are discussed as relevant to assembling composites for the aerospace industry (Ref. 25).

The work in this study was initiated to evaluate the weldability of four thermoplastic materials by three welding methods with the end goal being an assessment of weld strength, quality, repeatability, and factors which contributed to data variation such as edge effects, material influences, and weld area requirements. The three welding processes evaluated in this study are well established for joining thermoplastic composites and are used within the aviation industry. The intent of this study was not to rank these methods but rather identify the requirements and limitations of each method as (1) related to truss structure joints and (2) potential for in-space assembly.

Experimental

Materials

The thermoplastic materials welded within this study included three semicrystalline and one amorphous matrix composite. Material specifications are detailed in Table II.

Panel Manufacturing

Parent panels of each material were compression molded with a $[45/0/-45/90]_{2s}$ ply configuration according to supplier processing recommendations. Individual adherends for welding were machined from these panels at Cincinnati Test Laboratories using a diamond saw and TRIM E206 coolant. Adherends were cleaned with isopropanol prior to joining.

Single Lap Shear Coupon Welds

Adherend welding was contracted to three organizations with resistance welding performed at the National Institute of Aviation Research (NIAR) in Wichita, Kansas. Induction welding performed at Spirit Aerosystems in Wichita, Kansas, and ultrasonic welds were manufactured at Agile Ultrasonics in Columbus, Ohio. Adherend dimensions and single lap shear specimen sizes were manufactured to ASTM D5868 specifications; the standard test method for lap shear adhesion for fiber reinforced plastic (FRP) bonding.

TABLE II.—THERMOPLASTIC COMPOSITES SPECIFICATIONS AND SUPPLIERS

Resin	Fiber	Material designation	Vendor	Fiber areal weight, g/m^2	Resin weight percent, %	Ply thickness, mm
LM-PAEK	T700GC	TC1225	Toray	145	34	0.137
PEEK	AS4	TC1200	Toray	145	34	0.142
PPS	AS4	TC1100	Toray	221	34	0.210
PEI	AS4	APC	Toray/Solvay	145	32	0.132

Each organization was provided with adherends sufficient for both process development and test coupon welds. Optimization of process parameters was required for each material as physical material properties including matrix melt temperature, melt viscosity, and crystallization kinetics during cool down are expected to influence the welding process. Process development also addressed the weld area constraint imposed by the project, which was 2.54 by 2.54 cm (1 by 1 in.) for single lap shear (SLS) coupons, Figure 1.

The TDEA project elected to assess weldability on a per coupon basis rather than welding a single large part and machining out the required test coupons, Table III. Welding individual coupons allowed (1) an assessment of edge effects across each weld method and (2) a measure of reproducibility of weld quality by variation in lap shear strength (LSS). Nine SLS test coupons were manufactured per material and weld method. Six of those coupons were tested at NIAR and three were tested at NASA.

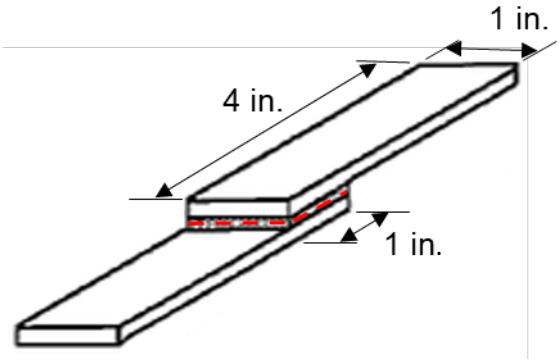

Figure 1.—Single lap shear specimen dimensions with weld area shown as red dashed lines.

TABLE III.—DISTRIBUTION AND COUPON REQUIREMENTS FOR RW, IW, AND UW

Material	Weld method	Weld organization	Process development coupons	Test coupons
T700/LM-PAEK	RW	NIAR	6	10
AS4/PEEK	RW	NIAR	6	6
AS4/PPS	RW	NIAR	6	9
AS4/PEI	RW	NIAR	6	8
T700/LM-PAEK	IW	Spirit AeroSystems	12	7
AS4/PEEK	IW	Spirit AeroSystems	12	9
AS4/PPS	IW	Spirit AeroSystems	12	9
AS4/PEI	IW	Spirit AeroSystems	12	9
T700/LM-PAEK	UW	Agile Ultrasonics	81	9
AS4/PEEK	UW	Agile Ultrasonics	81	9
AS4/PPS	UW	Agile Ultrasonics	81	9
AS4/PEI	UW	Agile Ultrasonics	81	9

All weld methods are sensitive to changes in substrates such as resin, fiber, and ply orientation. As such, it was necessary to adjust process parameters independently for each material system and weld configuration. Process variables and general process development procedures are detailed for each weld method. The optimization process included non-destructive evaluation (NDE) and cross-sectional imaging. Additional test coupons were welded and inspected for consolidation quality, crystallinity, and void content.

Process Development: Resistance Welding

A carbon fiber (CF) resistive element was selected for this work and placed at the interface between adherends. The CF insert was connected to a power supply and current was applied such that Joule loss generated sufficient heat to melt the thermoplastic resin at the bondline. Pressure was applied to consolidate the thermoplastic composite adherend. Pressure, resistance, voltage, current, and time were monitored and recorded throughout the process.

Process development coupons were used to determine the current required to melt each material based on the controllable process variables. Process development coupons of each material were initially welded with K-Type micro-thermocouples placed at the weld line to measure interface temperature, and the temperature data was used in the control loop. Data collected in this temperature control run were used to determine the power needed to reach the matrix melting temperature at the bond-line.

Once this data was acquired, a power curve was derived to allow for power control in subsequent welds. Additional welds were then performed using the power curve as the control variable, while still monitoring temperature at the interface. Multiple iterations were sometimes needed to achieve the target temperature, however, once the temperature response was acceptable a final check was made to verify the resistive element was still intact, i.e., fibers of the CF heating element had not shifted. This was done by confirming that the temperature control resistance and power control resistance were in agreement. If the temperature control resistance was not within a specified tolerance of the power control resistance the resistive element was considered defective. In this rare case, a new resistive element and weld stack was put into the setup and the process development was re-verified.

These process development steps were performed for each of the four materials welded in this study. A schematic of a general resistance welding configuration and photograph of the welding fixture at NIAR are provided in Figure 2.

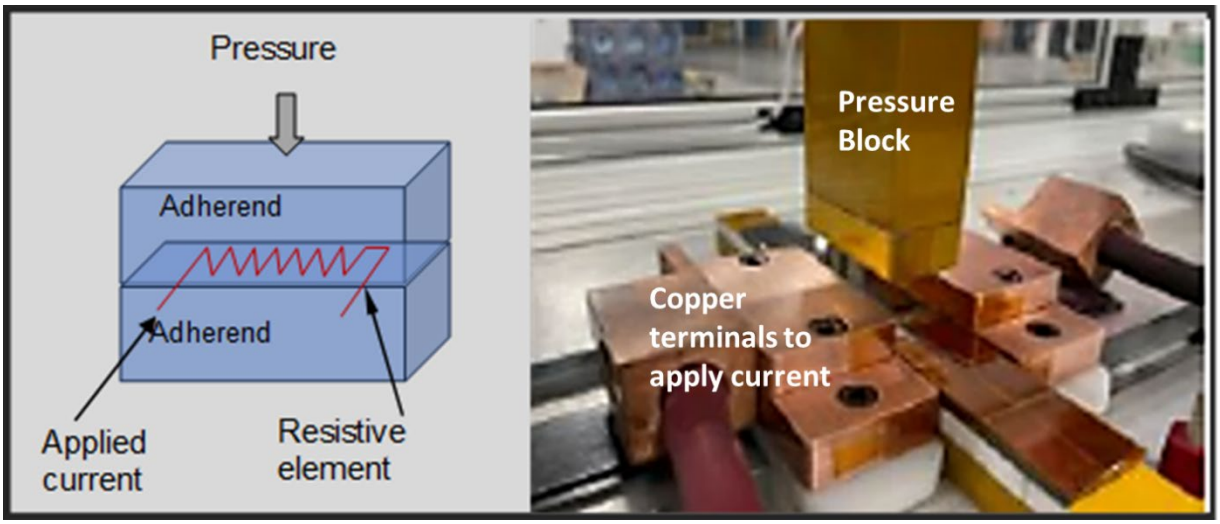

Figure 2.—Resistance welding schematic and equipment used for this study.

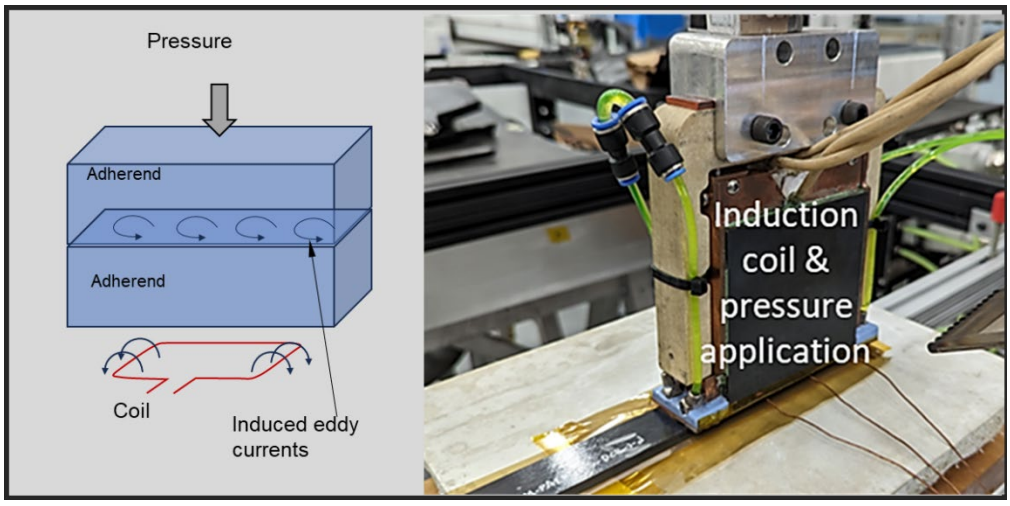

Figure 3.—Induction welding schematic and equipment used for this study.

Process Development: Induction Welding

When induction welding without a susceptor, the heat source is the carbon fiber inside the laminate. The carbon fiber conducts eddy currents induced by an induction coil, and the resultant Joule heating melts the surrounding thermoplastic resin to produce a weld. The magnitude of these currents and the resulting heat generation depends on several factors including conductivity of the fibers, proximity of the fibers to the coil, and orientation of fibers in adjacent lamina.

The two primary process parameters generally controlled to refine weld quality included applied current and cycle time. An increase of the applied current resulted in an increased magnitude of heat generated in the composite adherend and an increase in cycle time was found to increase the uniformity of temperatures at the weld line, due to conduction through the substrate.

A schematic of a general induction welding configuration and photograph of the welding fixture at Spirit Aerosystems is provided in Figure 3.

Process Development: Ultrasonic Welding

Ultrasonic welding uses high power ultrasonic frequencies to induce frictional heating. The implementation of UW used in this work followed two unconventional practices in preparation for scaling the process to large area welds. First, despite the relatively small target weld area, the sonotrode was translated across the part; referred to herein as a scan weld. Second, the welds were performed without using an energy director.

The primary process variables in ultrasonic welding include the sonotrode's peak-to-peak vibration amplitude, welding force (pressure), weld speed, and total cycle time. Prior to welding test coupons, Agile Ultrasonics performed a 3 by 3 full factorial design of experiments (DOE) to evaluate the influence of processing variables on strength and quality for each candidate material. The DOE included 81 welds per material and the lap shear strength was used to down-select process parameters.

A schematic of a general ultrasonic welding configuration and photograph of the welding fixture at Agile Ultrasonics is provided in Figure 4.

Process development detailed in the previous section yielded a manufacturing protocol for terrestrial joining. Modifications required for joining in-space or on the lunar surface have yet to be defined but the requirements for power and process time will be critical considerations for manufacturing in a lunar environment. Values for the power and process time used in this study are outlined in Table IV.

Figure 4.—Ultrasonic welding schematic and equipment used for this study.

TABLE IV.—POWER AND PROCESS TIME VALUES FOR THE THREE WELD METHODS EVALUATED

	Resistance welding	Induction welding	Ultrasonic welding, High amplitude	Ultrasonic welding, Low amplitude
Peak power, W	250	1000	2300	N/A
Average power, Ws	120	750	1600	250
Process time	7 to 8 min	40 to 60 s	3 s	30 s

In general, the power used for RW was relatively modest, likely due to the longer processing time and localized heating. Peak power for the weldability study welds was 250 W, and the average power was 120 W over the 7.5-min.-long welding process. The power required for IW with adherends having AS4 fibers was 500 to 1000 W. Active cooling of the induction coil may be required to mitigate overheating within the coupon, which adds to the power requirement. For UW coupons, a low amplitude, longer duration process had a modest power requirement of about 250 W (average). In contrast, high amplitude, short duration welds used about 1600 W average with peak readings around 2000 W. These power levels do not include heated tooling or sonotrode translation (for scan welds).

Weld Quality Inspection

Non-destructive evaluation (NDE) was performed on every welded specimen in the test matrix. A combination of pulse-echo ultrasonic C-scan (UT) and x-ray computed tomography (XRCT) was selected to characterize the state of the weld and adherends in the lapped region and in the heat affected zone adjacent to the welded area. Detailed analysis of the NDE will be presented in a companion technical memorandum (Ref. 26).

Photomicrographs enable visual inspection and defect analysis. Photomicroscopy was used to guide process optimization, and one traveler coupon per material was made specifically for photomicrography.

Single Lap Shear Tests

Lap shear strength (LSS) tests were performed both at NIAR and NASA, where NIAR tested six of the nine coupons welded per material/weld method and NASA tested the remaining three specimen per material/weld method. All specimens were gaged with four load introduction gages, mounted in back-to-back pairs and placed (1) centered on the overlap and (2) centered on a leg between the overlap and grip region. Additionally, two-inch extensometers with knife edges, were attached to each edge of the specimen and centered longitudinally on the overlap (to ±0.03 in.) to measure displacement across the

Figure 5.—L-brackets used to ensure alignment of SLS coupons during test.

joint. Specimens were tabbed to ensure proper alignment in the test fixture and a 2.54 cm (1 in.) grip length was used. L-Brackets, circled in Figure 5, were employed on the grips to ensure consistent gripping location.

All specimens were loaded and unloaded under stroke control. The displacement rate was set to 0.05 in. per minute so that the total loading duration was between 2 and 5 min from initial loading to specimen failure.

Results and Discussion

A summary of the lap shear strength per weld method is provided in Figure 6. The reported lap shear strength includes the six coupons tested at NIAR and 3 coupons tested at NASA.

The intent of this study is not to rank the weld methods, however, the overall comparison of the LSS cannot be ignored. RW yielded the highest LSS for three of the four materials. However, the relative performance of RW may speak to the constraints of this study, with RW better suited for the coupon dimensions that were provided. For example, considering the small weld area, edge effects likely had a greater influence in the IW and UW coupons than RW coupons. It is also noted that material/weld combinations for which the welding organization had significant previous experience tended to have higher LSS. For example, RW for the SLS configuration examined here has been used through hundreds of welding trials prior to this work especially for PEEK and LM-PAEK. In contrast, most of the previous work for UW and IW have focused on welding larger panel sizes where edge effects are less important. UW had the lowest LSS for three of the four materials, which may be related to the scan welding process that was used rather than static welds, and the absence of an energy director. Overall, the LSS measured

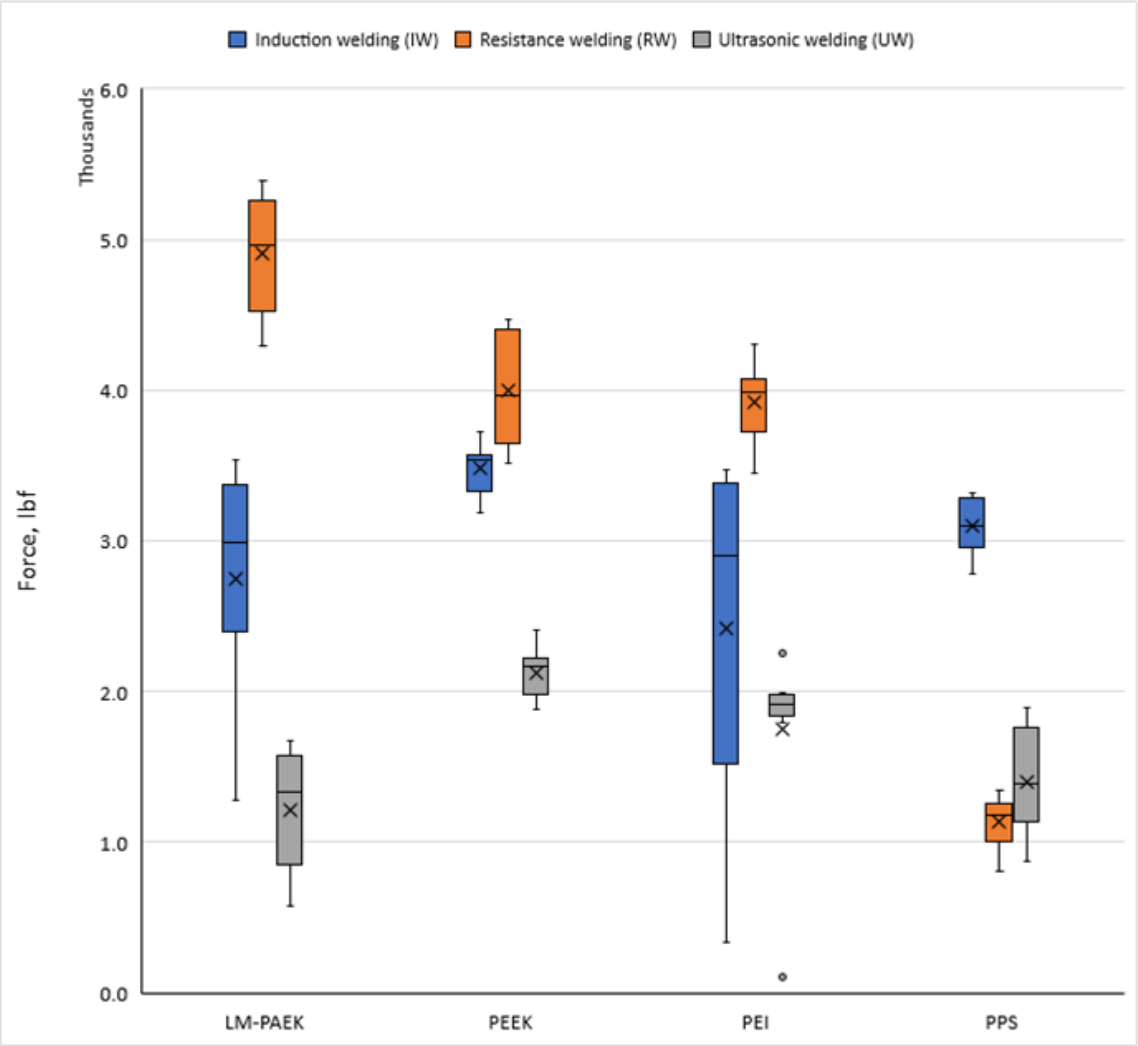

Figure 6.—Summary of the LSS strengths from the weldability study. The number of replicates for each case was 9 except where indicated by a number above the dataset. The mean values are indicated with x symbols and outliers are shown with circular markers.

within this study tended to be lower than values reported in the literature (Refs. 27 and 30), which was attributed to inadequate process development (i.e., non-optimal process settings), welding without an energy director, and welding individual specimens (i.e., edge effects). Additional details on the influence of these process considerations will be addressed in the following sections.

Coefficient of Variation (COV)

The TDEA project set a reproducibility target of <10% COV in the LSS data at the outset of this study, Figure 7. Three of the four RW materials met this criterion. Two of the four IW and UW specimen met the COV target. There was not a clear trend indicating a material influence on reproducibly of weld quality or lap shear strength. LSS data presented in Figure 6 shows a single datapoint contributing to the high COV, for example the IW/PEI dataset. However, in most instances, the COV represented data scatter without a clear outlier.

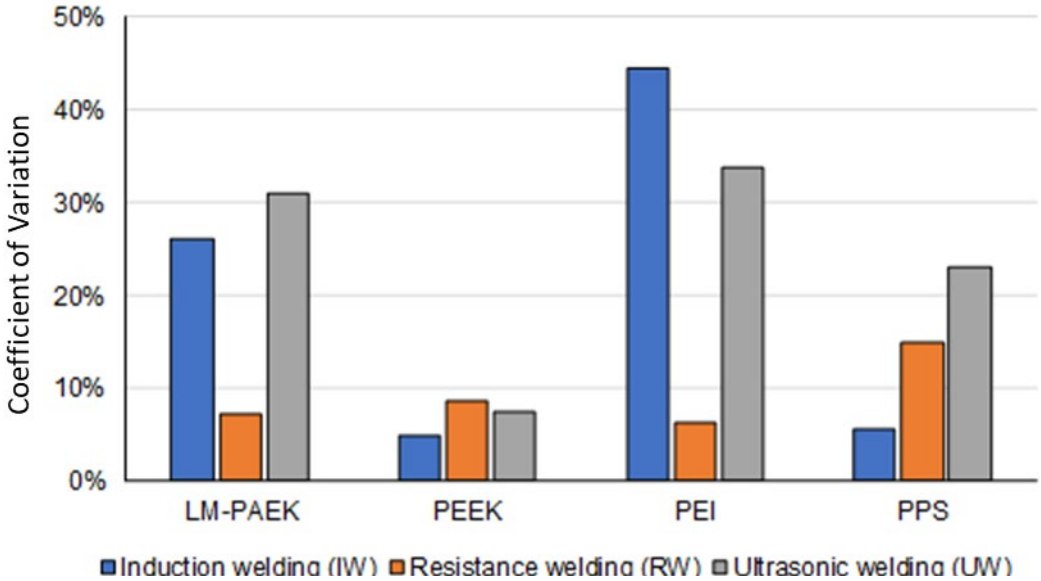

Figure 7.—Coefficient of variation in lap shear data for each material and weld process, based on SLS tests at NIAR only, n = 6.

Non-Destructive Evaluation

Several defects were observed throughout this study which contributed to the relatively low LSS and high COV in some material/weld combinations. While variability in the LSS data provided a metric for reproducibility, the underlying issue was in the reproducibility of the weld itself, i.e., following a single process for nine welds did not necessarily result in nine welds of similar quality. Variation in bond quality can be visualized through C-scan images where dark regions represent areas of high attenuation and thus poor consolidation in the weld area. Figure 8 to Figure 10 show NDE results for several LM-PAEK specimens welded by RW, IW, and UW and the results show significant variations among the specimens.

For RW, the variance in weld strength, despite following the same process, is likely due to inconsistencies in the resistive element, such as fiber distortion occurring during coupon loading or defects in the resistive elements. These issues can lead to uneven temperature distribution with potential under- or over-heating, which in turn causes uneven pressure during the weld. Therefore, while the process may be standardized, numerous factors must be tightly controlled to achieve a consistent, reproducible weld quality.

NDE of the IW LM-PAEK is shown in Figure 9, with the weld area outlined in red. NDE of these coupons exhibited significant attenuation, and this was supported by the visual assessment of the quality of the coupons, which showed surface blistering and deconsolidation. Areas of attenuation extend outside the overlapped region into the adherends as indicated by an arrow in the figure. The variability observed in the LM-PAEK specimens is partially attributed to edge effects resulting from the increased applied currents necessary to achieve a weld with the T700 fibers (as compared with AS4 fibers). While means of mitigating edge effects were in place, for most materials edge effects were reduced by utilizing a lower current. These edge effects primarily presented as arcing and degradation of the laminate or unwelded areas.

NDE of UW LM-PAEK also showed considerable attenuation, Figure 10, which was attributed to processing constraints defined by the project. The variability in the results can be partially explained by sensitivity of frictional heating to small differences in material microstructure and surface condition. Variability was also attributed to challenges with temperature control throughout the weld process and the need for fixture optimization to mitigate edge effects.

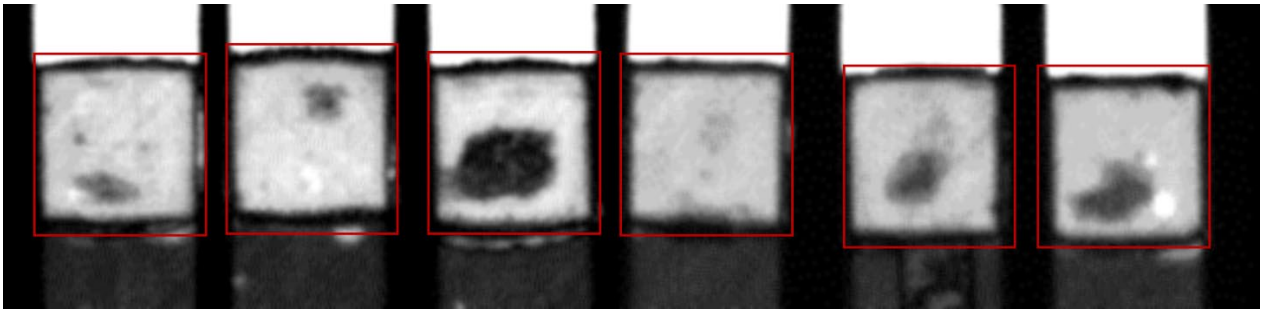

Figure 8.—NDE of resistance welded LM-PAEK (6 specimens, loading direction is vertical).

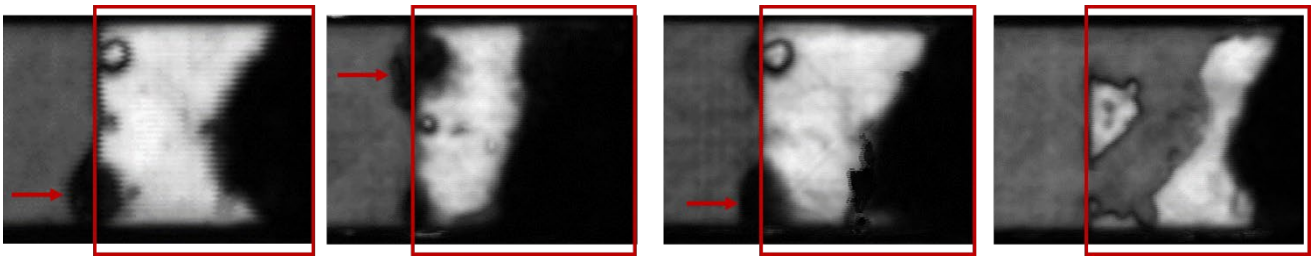

Figure 9.—NDE of induction welded LM-PAEK reveals partial bonding (4 specimens, loading direction is horizontal).

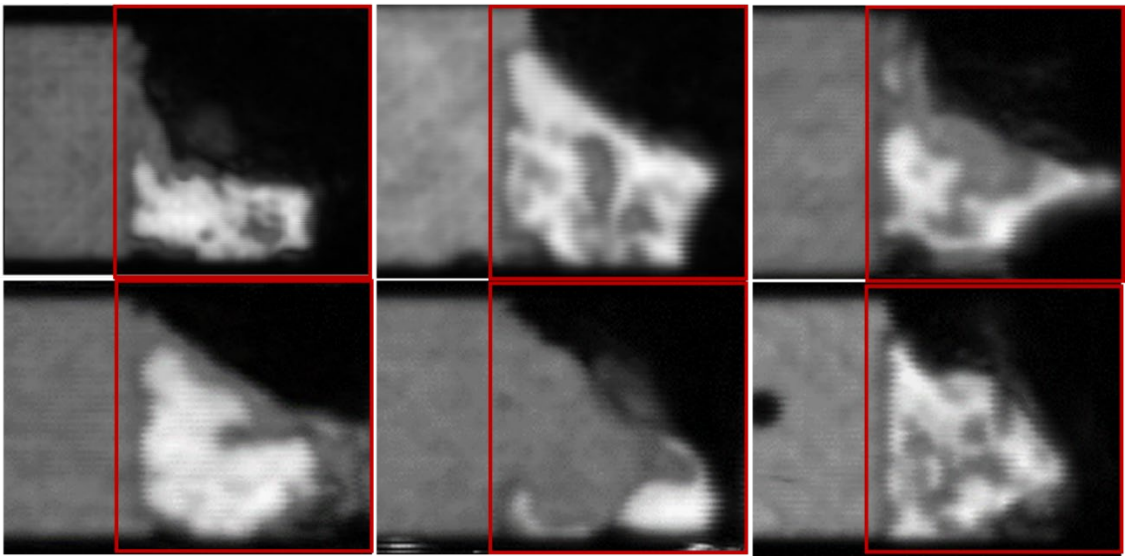

Figure 10.—NDE of ultrasonically welded LM-PAEK reveals partial bonding (6 specimens, loading direction is horizontal).

Fracture Surface Analysis

Post-test fracture surface assessments are consistent with the LSS, COV, and NDE findings. Figure 11 shows representative SLS failure surfaces associated for each material and weld method evaluated. The load direction is left to right for the image set.

RW failure surfaces show the carbon fiber tows used as a heating element, which are oriented perpendicular to the coupon length. Fiber tows can be seen on both adherend sides, supporting an assessment of good fusion to both adherends. The presence of fiber tows from the heating element across the full weld area, contribute to uniform heating and ultimately higher strength and lower COV of the coupons manufactured by RW. A drawback of additional 90-degree tows at the bondline is that tows will typically fail first under tensile loading, representing a weakness that may contribute to failure initiation in these coupons.

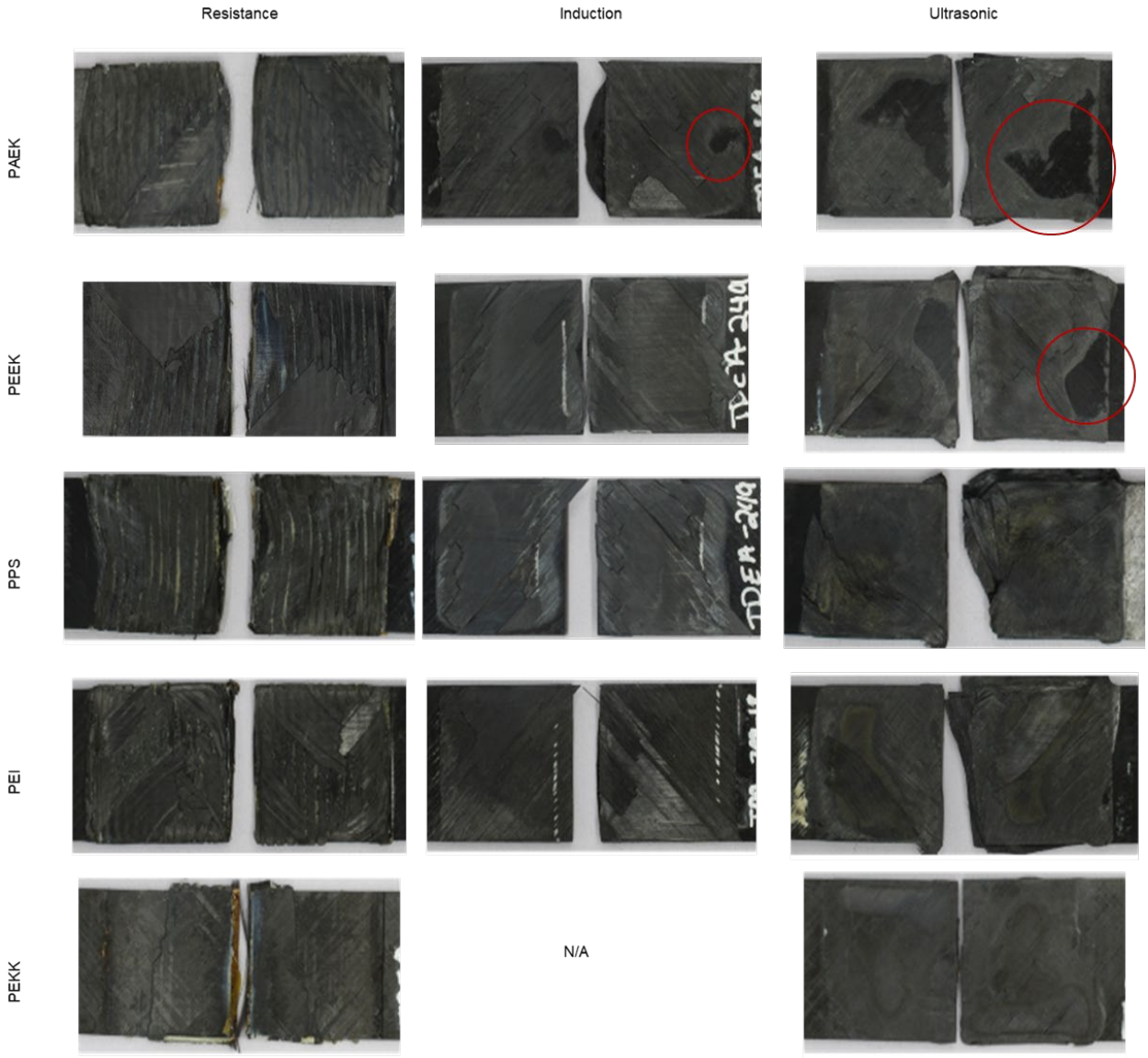

Figure 11.—Fracture surfaces following single lap shear tests of each material welded by RW, IW, and UW.

Most prominent in the IW and UW fracture surface images is the lack of weld consistency across all materials. Fracture surfaces of LM-PAEK and PEEK in these weld types have dark areas (circled) indicative of material that was not fused in these regions. In cases where more full fusion is evident, the coupon edges show fiber washout and non-uniformity in the weld edge. A curved path that appears un-fused can be seen in the PPS IW and UW coupon failure images. The lack of consistency in those weld edges is consistent with NDE (Figure 7) and, as previously mentioned, amplify peel force reactions leading to lower strength and higher COV.

On the positive side, IW and UW hold promise. These welds are significantly faster than RW and can use much less energy per weld. There is evidence that some areas fused well and showed good failure modes. With more development it is reasonable to expect edge welds to be more complete with less adherend defects leading to welds as strong as the resistance weld with lower COV.

Defects Common to All Weld Methods

Ideally, heat required for joining is limited to the bonding surfaces, however regions of the laminate adjacent to the bond area often experience a rise in temperature. Ideally this heat affected zone is as close to the bonding surface as possible to reduce unintended defect formation (Ref. 31). For resistance and induction welds, heat is concentrated at the bondline but can conduct through adjacent plies and outward into the adherend. For ultrasonic welding, in particular without an energy director, heat is generated through the thickness of the adherend in contact with the sonotrode. Representative photomicrographs show the cross-sectional region of lap shear coupons for each material and weld method, Figure 12. Common defects within the heat affected zone were observed across all weld methods and include fiber pushout, porosity, delamination, incomplete welds and variation in adherend thickness. In some cases, such as ultrasonically welded PPS, polymer degradation during the weld process led to significant delamination in the bond region.

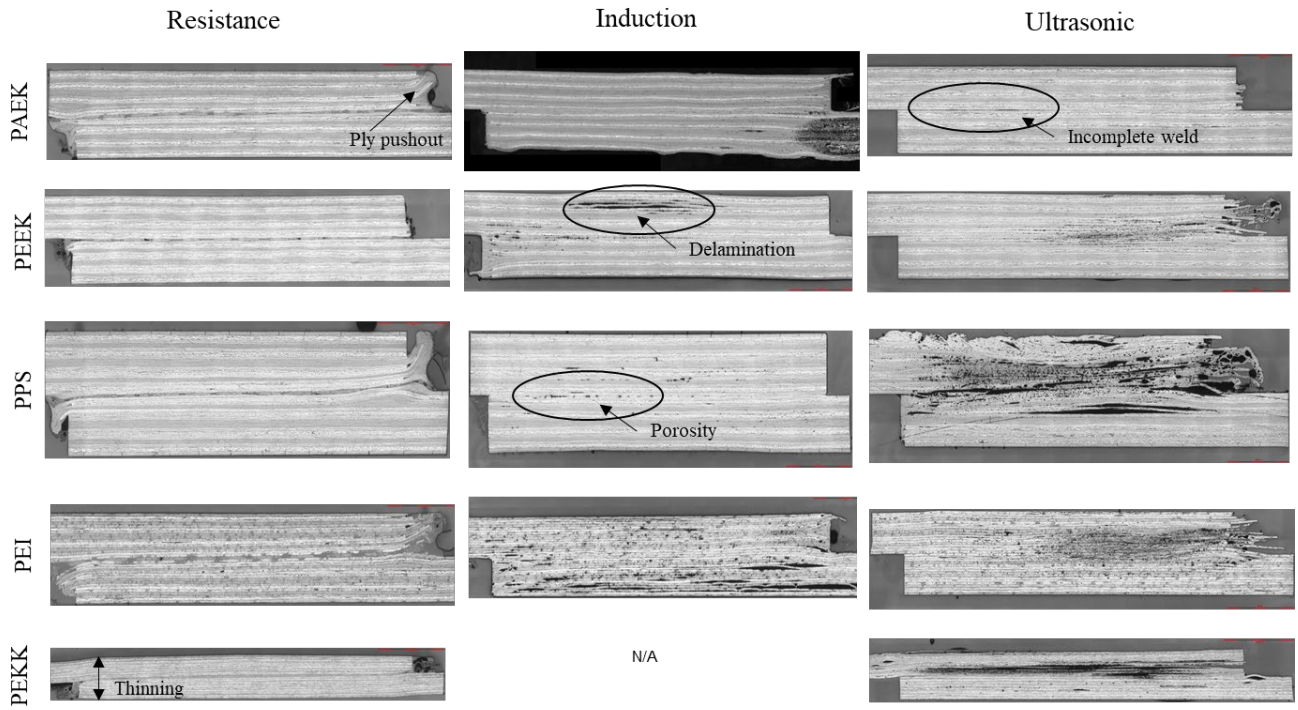

Figure 12.—Photomicrograph of AS4/PEI joined by resistance welding.

Ply pushout due to pressure applied above the matrix melt temperature was observed across all weld methods. Fiber movement is common during thermoplastic composite processing as embedded carbon fiber is carried in the flow of molten thermoplastic matrix when held under pressure. Other common defects included voids and delamination and are primarily due to insufficient pressure on the part during cooling. Void content in test coupons varied based on material and weld method as indicated by C-scan data presented in the previous section.

Finally, all welding organizations reported seeing smoke during process development welds, indicating polymer degradation which can lead to void formation and reduced bond strength. This was largely mitigated through process optimization.

Role of Edge Effects

The design of the lap shear coupon leads to peel stresses which are most concentrated at the edges of the test specimen (Ref. 32). Because the failure mode of the SLS test compounds the influence of edge defects, welds that did not extend to the coupon edge were important to note. High speed images collected during the lap shear tests confirms failure initiation at the edge, Figure 13.

Resistance Welding

NDE presented in Figure 8 shows that coupons welded by resistance welding are well consolidated near the edge, and as a result LSS data of RW coupons best met reported values.

Induction Welding

Edge effects are typically observed when induction welding is performed near an edge of a laminate as the edge serves as a concentration for return currents leading to localized overheating and defects. The individual coupons welded in this study included several edges under the work head, and therefore significant edge effects were observed. To reduce edge effects, modifications to the initial fixture design were made.

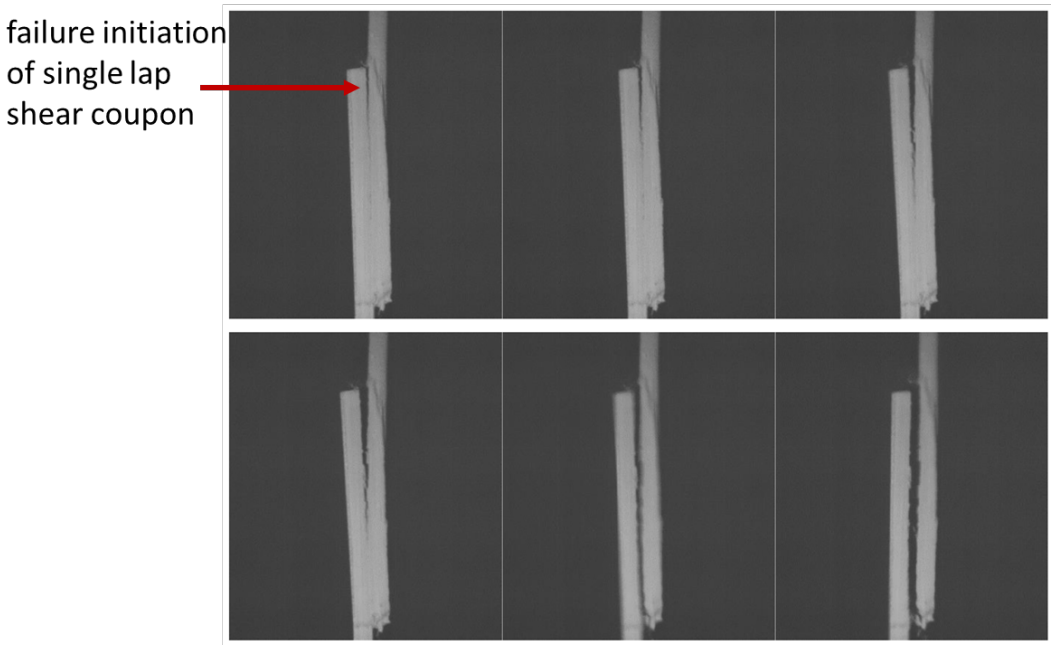

Figure 13.—Typical failure progression of a single lap shear tests with failure initiating at the edge of the bonded area.

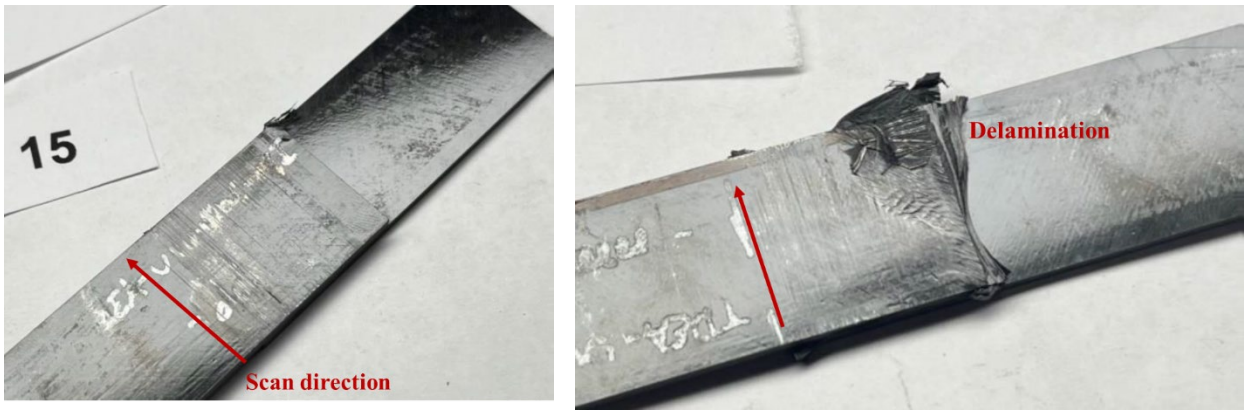

Figure 14.—Ultrasonic scan welding has the potential for edge defects such as delamination.

Ultrasonic Welding

Edge effects in scan welding with ultrasonics are due to nonoptimal weld time and/or pressure, in particular at the start and stop location of the sonotrode. Scan lines observed on the surface of the bond area, Figure 14, result from the sonotrode moving across the specimen. Fiber pushout on the edges can be observed in some cases during the process development welds. Ultrasonic welding of thermoplastic composites is generally used for spot welding a relatively small area. However, to weld large structures there is a need to develop continuous ultrasonic welding. Successful continuous welds have been reported by translating the sonotrode along the line to be welded (Ref. 33). The continuous or scan weld requires particular attention to pressure at throughout the process, and time spent at each location. These factors are exacerbated at the start stop locations, and lead to significant edge effects in the 2.54 by 2.54 cm area constraint of these coupons.

Role of Fiber Type in Induction Welding

The fiber type plays a role primarily in induction welding. In this study, three of the four materials used AS4 fibers, while the fourth has T700 fibers (LMPAEK/T700). Prior experience with this fiber type suggested it can prove challenging to reliably produce an induction weld due to the relatively lower electrical conductivity of T700 fibers.

The lower electrical conductivity of the T700 fibers results in significantly reduced heating of the substrate for a given applied current when compared to similar layups and thicknesses of other fiber types. This typically results in a need for increased applied currents to achieve a weld. Therefore, trials performed with LM-PAEK/T700 specimens required significantly higher applied currents to achieve processing temperatures. However, the high output current resulted in surface defects throughout the adherends, likely due to undesired heating outside the overlap region. Across several pairs of adherends, process parameters were gradually increased to result in an adequate welded region. The process parameters that successfully produce a weld resulted in significant visual defects, as seen in Figure 15.

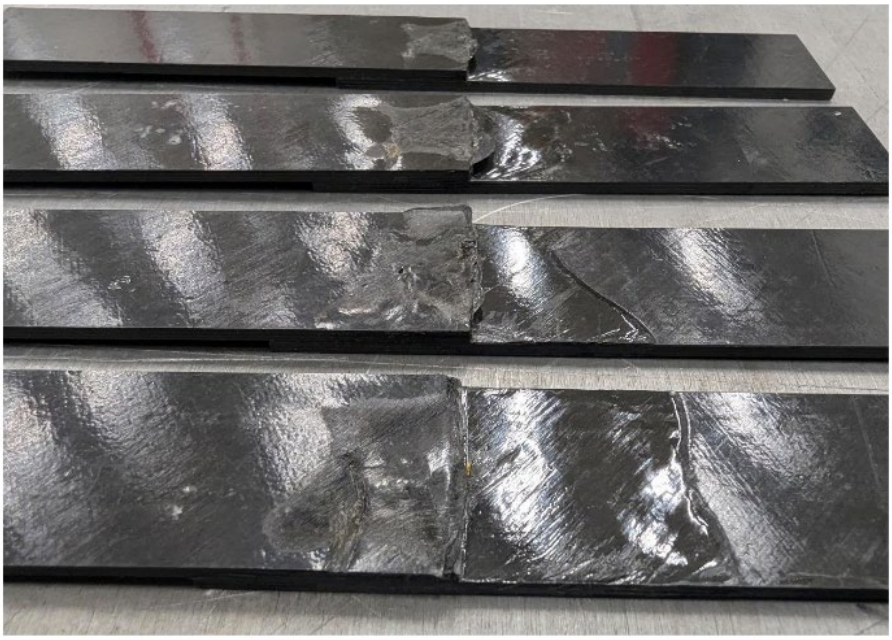

Figure 15.—Visual defects present on LM-PAEK induction-welded SLS coupons.

Summary

Single lap shear coupons for four candidate thermoplastic composite materials (AS4/PEEK, AS4/PPS, T700/LM-PAEK, and AS4/PEI) were joined by resistance, induction, and ultrasonic welding. The goal of the study was an evaluation of each weld process with respect to bond strength, bond quality, reproducibility of the weld process, and limitations based on specimen size or material. Several common defects and material/process specific defects were noted including edge effects due to the coupon size. In general, test data generated from coupons that were resistance welded met the <10% COV goal of the project for three of the four materials in the test matrix. Induction and ultrasonic welded coupons met the COV goal for two of the four materials. The data indicates the requirement for process development per material and in particular for the constraints imposed by a part design.

References

1. J.T. Hoggatt and M. Kushner, “Applicability of thermoplastic composites for space structures,” in Langley Space Systems Technology Seminar, Hampton, VA, 1978.
2. E.M. Silverman, R.A Griese, and W.C. Forbes, “Property performance of thermoplastic composites for spacecraft systems,” *SAMPE Journal*, vol. 25, no. 6, pp. 38–47, 1989.
3. R.E. Garvey, “Potential for advanced thermoplastic composites in space systems,” in *International technical conference of the Society for the Advancement of Material and Process Engineering*, Boston, MA, 1990.
4. A.R. Chadwick, P. Dreher, I. Petkov, and S. Nowotny, “A fibre-reinforced thermoplastic primary structure for sounding rocket applications,” in *SAMPE Europe Conference 2019*, Nantes-France, 2019.
5. D.M. Grogan, C.M. O’Bradaigh, J.P McGarry, and S.B. Leen, “Damage and permeability in tape-laid thermoplastic composite cryogenic tanks,” *Composites: Part A, Applied Science and Manufacturing*, vol. 78, pp. 390–402, 2015.

6. J. Dolan, A. Doyle, C.M. Ó Brádaigh, D. Jaredson, "Out-of-Autoclave Manufacturing of Large Integrated Structures Using Thermoplastic Composite Materials," ECCM15 - 15TH European Conference on Composite Materials, Venice, Italy, 24–28 June 2012.
7. C. Semprimoschnig, "Overview of advanced materials and surface activities at ESA," in *EIROFORUM WAMAS* meeting, CERN, November 19–20, 2013.
8. G. Gardiner, "Precision Design for Deployable Space Structures," *CompositesWorld*, June 2016, pp. 46.
9. "On Orbit Assembly and Manufacturing State of Play, 2021 Edition," Page 72 https://ntrs.nasa.gov/api/citations/20210022660/downloads/osam_state_of_play%20(1).pdf
10. NASA Technology Demonstration Missions website, "On-orbit servicing, assembly, and manufacturing 2 (OSAM-2)," https://www.nasa.gov/mission_pages/tdm/osam-2.html
11. B. Diehl and SM. Kothe, "Investigation of Innovative Technologies for Automated Assembly and Joining of a Full-Scale Thermoplastic Composite Fuselage," AIAA 2024-0876.
12. Airbus press release, "Fantastic Thermoplastics," January 2025. https://www.airbus.com/en/newsroom/stories/2025-01-fantastic-thermoplastics
13. R.P. Wool, B.-L. Yuan and O.J. McGarel, "Welding of polymer interfaces," *Polymer science and engineering,* vol. 29, no. 19, pp. 1340–1367, 1989.
14. A. Beevers, "Welding: the way ahead for thermoplastics?" *Engineering* vol. 231, pp. 11–12, 1991.
15. T.J. Ahmed, D. Stavrov, and H.E.N Bersee, "A comparison of fusion bonding techniques: resistance and induction welding," *In: Proceedings of the SAMPE Europe International Conference*, Paris, France, 2005, pp. 111–116.
16. A. Benatar and T.G. Gutowski, "Methods for fusion bonding thermopastic composites, *in SAMPE Quarterly*, vol. 18, no. 1, pp. 35–42, 1986.
17. I.Y. Chang and J.K. Lees, "Recent development in thermoplastic composites: a review of matrix systems and processing methods," *Journal of Thermoplastic Composite Materials*, vol. 1, pp. 277–296. 1988.
18. F.N. Cogswell, P.J. Meakin, A.J. Smiley, M.T. Harvey, and C. Brooth, "Thermoplastic Interlayer Bonding for Aromatic Polymer Composites," *In: Proceedings of the 34th International SAMPE Symposium*, pp. 2315–2325, 1989.
19. K.C. Cole, "A review of recent Developments in joining high-performance thermoplastic composites," *In: Proceedings of Canadian International Composites Conference and Exhibition*, pp. 341–348, 1992.
20. R.A. Grimm, H.J. Yeh, and G.W. Ritter, "Joining of composites," *Composites Manufacturing*, vol. 12, no. 4, pp. 1–6, 1992.
21. M.C. Li and A.C. Loos, "The effects of processing on interply bond strength of thermoplastic composites," *Journal of Reinforced Plastics and Composites,* vol. 11, pp. 1142–1162, 1992.
22. C.A. Butler, R.L. McCullough, R. Pitchumani, and J.W. Gillespie Jr, "An analysis of mechanisms governing fusion bonding of thermoplastic composites," *Journal of Thermoplastic Composite Materials*, vol. 11, pp. 338–363, 1998.
23. I.F. Villegas, L. Moser, A. Yousefpour, P. mitschang, and HE Bersee, "Process and performance evaluation of ultrasonic, induction and resistance welding of advanced thermoplastic composites," *Journal of Thermoplastic Composite Materials*, vol. 26, no. 8, pp. 1007–1024, 2012.
24. C. Ageorges and L. Ye, "State of the art in fusion bonding of polymer composites," *In: Fusion Bonding of Polymer Composites. Engineering Materials and Processes*. Springer, London. 2002.

25. A. Korycki, C. Garnier, M. Bonmatin, E. Laurent and F. Chabert, “Assembling of carbon fibre/PEEK composites: comparison of ultrasonic, induction, and transmission laser welding,” Materials, vol. 15, pp. 6365, 2022.
26. P.H. Johnston, et al., “Non-destructive and destructive analysis of welded single-lap shear thermoplastic composites,” NASA Technical Memorandum, in preparation, 2025.B.
27. Jongbloed, J. Teuwen, R. Benedictus, I.F. Villegas, “On differences and similarities between static and continuous ultrasonic welding of thermoplastic composites,” *Composites Part B*, vol. 203, (2020), 108466.
28. W.P. Seneviratne, J.S. Tomblin, B.L. Saathoff, “Influence of various surface preparation techniques on resistance welded and adhesively bonded unidirectional thermoplastic composite joints,” *SAMPE Conference Proceedings*, 2021.
29. H. Shi, I.F. Villegas, and H.E.N. Bersee, “Strength and failure modes in resistance welded thermoplastic composite joints: Effect of fibre-matrix adhesion and fibre orientation,” *Composites: Part A*, vol. 55, pp. 1–10, 2013.
30. T.J. Ahmed, D. Stavrov, H.E.N Bersee, and A. Beukers, “Induction welding of thermoplastic composites – an overview,” *Composites: Part A* vol. 37, pp. 1638–1651, 2006.
31. D. Stavrov and H.E.N Bersee, “Resistance welding of thermoplastic composites – an overview,” *Composites: Part A* vol. 36, pp. 39–54, 2005.
32. I.F. Villegas and R. Calvin, “The dangers of single-lap shear testing in understanding polymer composite welded joints.” *Philosophical Transactions of the Royal Society A* 379.2203 (2021): 20200296.
33. F.S. Senders, M. van Beurden, G. Palardy, and I.F. Villegas, “Zero-flow: a novel approach to continuous ultrasonic welding of CF/PPS thermoplastic composites plates,” Advanced Manufacturing: Polymer & Composites Science, 2016.